Available at
http://pvamu.edu/aam
Appl. Appl. Math.
ISSN: 1932-9466

Applications and Applied Mathematics:
An International Journal
(AAM)

Vol. 9, Issue 1 (June 2014), pp. 186-200

Modelling the Flow of Aqueous Humor in Schlemm's Canal in the Eye

Ram Avtar, Swati Srivastava, Rashmi Srivastava
Department of Mathematics
Harcourt Butler Technological Institute
Kanpur 208002, India

Received: November 21, 2013; Accepted: April 21, 2014

Abstract

A simple mathematical model for the transient flow of aqueous humor in the canal of Schlemm is developed to investigate the acceleration effects of a sudden elevation in the intraocular pressure on the flow characteristics of the aqueous humor in the canal. The model treats a canal segment as a tube of elliptic cross-section. Exact analytical solution to the model is obtained using separation of variables method. The effects of some important model parameters on the maximum and minimum shear stresses exerted on the Schlemm's canal epithelial cells (wall) by flowing aqueous humor are investigated for the steady-state flow.

Keywords: Schlemm's canal; Intraocular pressure; Aqueous humor.

MSC (2010) No.: 34A99, 76B99

1. Introduction

A colorless intraocular fluid, aqueous humor, is secreted by the ciliary epithelium, flows in the posterior chamber bathing the lens, through the iris, in the anterior chamber providing a transparent medium and nutrients to the avascular tissues, and pressurizing the eye and then drains into the venous system through the trabecular meshwork and the canal of Schlemm.

Most of the anomalous process as occurring inside the canal of Schlemm tends to elevate the intraocular pressure (IOP) by preventing the exit of aqueous humor and representing a pathological state of the eye, known as open angle glaucoma. If there is a sudden rise in the intraocular pressure in the anterior chamber, the percolation of aqueous humor in the Schlemm's canal through trabecular meshwork may be accelerated and this instantaneous acceleration may affect the flow of aqueous humor in the canal of Schlemm.

Schlemm's canal is a small collecting duct lined by a monolayer of vascular-derived endothelial cells [Hamanaka et al. (1992) and Krohn (1999)]. The Schlemm's canal endothelial (SCE) cells probably play a role in determining IOP [Ethier (2002)]. SCE cells on opposite sides of the canal are sometimes observed to be very well aligned with one another. The mechanism of such alignment is not clearly understood. The alignment of SCE cells, under the pathological state, may contribute to the outflow resistance increase. The knowledge of the factors ensuring SCE cells alignment may be of interest and important in the understanding of the common ocular disease, glaucoma. Shear stress exerted by flowing aqueous humor within Schlemm's canal plays a key role in the alignment of SCE cells and may be one of the factors that control IOP.

A great wealth of experimental work available in the ophthalmic literature [Nesterov (1970 a, b), Johnson and Grant (1973), Van Buskirk (1982), Ethier (2002)] show that increasing IOP produces progressive collapse of Schlemm's canal. Johnson (1983) developed a mathematical model of Schlemm's canal to simulate the collapse of the canal and its resistive effect on the aqueous outflow. Tandon and Autar (1989) proposed a mathematical model for the flow of aqueous humor in the Schlemm's canal with porous upper wall and concluded that increased IOP or decreased rigidity of the inner wall may contribute to the development of increased resistance and that increasing values of filtration constant may contribute to the facility of outflow increase. A theoretical model for the flow in Schlemm's canal was developed by Either et al. (2004) to estimate shear stresses applied to endothelial cells by flowing aqueous humor and concluded that SCE cells experience physiologically significant levels of shear stress, promoting cell alignment which may help to control the caliber of Schlemm's canal. Avtar and Srivastava (2006) developed a mathematical model which treated the Schlemm's canal as a porous compliant channel that is held open by the trabecular meshwork and studied the aqueous fluid pressure and flow profiles in the proposed model. Ismail and Fitt (2008) proposed a mathematical model for the flow of aqueous humor through the trabecular meshwork and into the canal of Schlemm and coupled the flow to the pressure in the anterior chamber in order to predict changes in IOP.

Initially, the steady-state of aqueous flow prevails, a sudden elevation in IOP may increase pressure drop across the trabecular meshwork causing a sudden application of extra pressure gradient on the aqueous percolation in the Schlemm's canal. As a result of sudden application of extra pressure gradient, a time dependent problem may be observed. The purpose of present piece of research work is to investigate theoretically the transient changes, if any, in the characteristics of the circumferential flow of aqueous humor in the canal of Schlemm as a result of sudden application of a pressure gradient due to sudden elevation in IOP. This paper is concerned with the development of a mathematical model for the flow of aqueous humor in the canal of Schlemm and with the analysis of sensitivity of flow characteristics to the time. Effects of various important model parameters on the shear stresses experienced by SCE cells (wall) applied by steady state flow of aqueous humor in the canal of Schlemm have been represented through graphs and discussed.

The novelty of the present piece of work is that the effects of some model parameters: IOP, the filtration constant, and the minor axis on the minimum and maximum wall shear stresses exerted on SCE cells by the flowing aqueous humor is being investigated. To the best of our knowledge, none of the previous research papers has addressed/conducted such analytical investigation.

2. Model Description

Most of the aqueous humor that percolates in the Schlemm's canal through the trabecular meshwork must flow some distance along the canal to reach a collector channel. A canal segment between the two collector channels is treated as an elliptical channel. Half of the surface of the elliptical channel in contact with the trabecular meshwork is porous. Almost half of the amount of aqueous humor entering into the canal segment approaches the collector channel to the right of the midpoint between two collectors and other half to the left. Due to the symmetry conditions, the flow of aqueous humor is considered for present study in right half of the segment along x-axis. Thus, the aqueous flow along the canal segment is considered as a fluid flow through a narrow tube with elliptical cross-section.

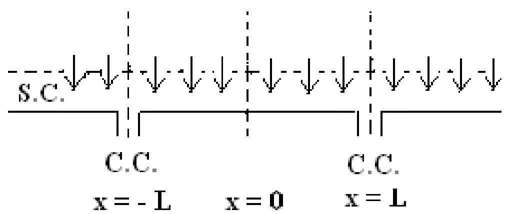

Figure 1. Schematic diagram of the segment of canal of Schlemm

Assumptions

The inner endothelium wall of the canal which is in contact with the trabecular meshwork is porous and collapsible. The flow of aqueous humor is laminar, Newtonian, viscous, and incompressible. The inner wall of Schlemm's canal deforms in proportion to local pressure drop across it. All collector channels are equidistant and of the same size, and the same amount of the aqueous humor is drained by each channel.

Governing Equations

The Navier-Stokes equation which is a partial differential equation expressing the local balance of the momentum in a fluid around any point of space at any time is given by-

$$\rho \frac{D\bar{u}}{Dt} = -\bar{\nabla} p + \mu \bar{\nabla}^2 \bar{u} + \bar{f},$$

where the term $\frac{D\bar{u}}{Dt}$ is the instantaneous acceleration, $-\nabla p$ is the dynamic pressure gradient, $\mu\bar{\nabla}^2 \bar{u}$ is the shear viscosity term, and $\bar{f}$ is the external body force and here we assume that there is no external force and $\bar{u} = (u, 0, 0)$.

Introducing the assumptions mentioned above, the governing Navier-Stokes equations reduce to:

$$\frac{\partial u}{\partial t} = -\frac{1}{\rho}\frac{\partial p}{\partial x} + \nu \nabla^2 u, \tag{1}$$

$$-\frac{\partial p}{\partial y} = 0, \tag{2}$$

$$-\frac{\partial p}{\partial z} = 0, \tag{3}$$

where ν is the kinematic viscosity.

The equation of continuity is

$$\frac{\partial u}{\partial x} = 0. \tag{4}$$

Since the second and third equations show that the pressure is a function of x at most and the velocity is a function of y and z at most, both the pressure gradient and the viscous term must equal a constant.

The unsteady problem given in equation (1) is converted into steady-state and transient problems using the transformation

$$u = u_s + u_t. \tag{5}$$

In the steady-state case, u_s is independent of t and $\frac{\partial u_s}{\partial t} = 0$. Thus, the steady-state problem is obtained in the form:

$$\frac{\partial^2 u_s}{\partial y^2} + \frac{\partial^2 u_s}{\partial z^2} = \frac{1}{\mu}\frac{dp}{dx}, \tag{6}$$

and the unsteady part is given by:

$$\frac{\partial u_t}{\partial t} = \nu\left(\frac{\partial^2 u_t}{\partial y^2} + \frac{\partial^2 u_t}{\partial z^2}\right). \tag{7}$$

The partial differential equation (7) is of parabolic type. According to the steady-state material balance in the infinitesimal element of the canal segment:

$$w(x)\,dx = q(x+dx) - q(x), \tag{8}$$

where $w(x)$ represents the filtration flux of the aqueous humor per unit length, and $q(x)$, the aqueous volume flux in the canal.

Expanding $q(x+dx)$ in a Taylor series:

$$\frac{dq(x)}{dx} = w(x), \tag{9}$$

where

$$q(x) = \iint u_s \, dydz, \tag{10}$$

$$\mathrm{w(x) = G[P}_I - \mathrm{p(x)]}, \tag{11}$$

where G is the filtration constant of the porous wall and P_I is the intraocular pressure.

Solution to the steady-state problem

The canal segment along which the aqueous humor is flowing is treated as a narrow tube which has an elliptical cross-section with semi-axes a and b. The physically realistic and mathematically consistent boundary conditions for the steady-state problem are prescribed as follows:

$$u_s(y,z) = 0 \quad \text{around the inner perimeter,} \tag{12}$$

$$p(x = L) = P_o, \tag{13i}$$

$$\left.\frac{dp}{dx}\right|_{x=0} = 0, \tag{13ii}$$

where P_o is the pressure at the mouth of the collector channel.

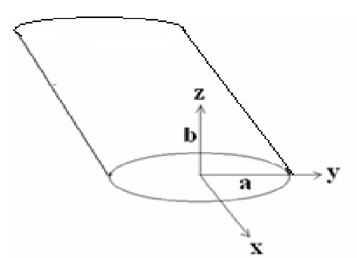

Figure 2. Schematic diagram of the canal segment with elliptic cross-section

Although there are many different approaches to solve the linear partial differential equation (6), here we shall consider a very simple, yet powerful approach to solve the full non-homogenous equation. Note that the solution u_s must satisfy the no-slip flow boundary condition around the inner perimeter. Consequently, let us consider a function $g(y,z)$ that is zero over the entire boundary of the flow, which for the elliptical boundary is

$$u_s = k\left(\frac{y^2}{a^2}+\frac{z^2}{b^2}-1\right), \tag{14}$$

where k is an unknown parameter.

Using equation (14) in equation (6), we find

$$k = \frac{1}{2\mu}\left(\frac{a^2b^2}{a^2+b^2}\right)\frac{dp}{dx}. \tag{15}$$

Substituting the value of k in equation (14), we find

$$u_s = \frac{1}{2\mu}\left(\frac{a^2b^2}{a^2+b^2}\right)\left(\frac{y^2}{a^2}+\frac{z^2}{b^2}-1\right)\frac{dp}{dx}. \tag{16}$$

Now, the aqueous outflow is given by:

$$\mathrm{q(x)} = \iint u_s dydz = -\frac{\pi ab}{2}k, \tag{17}$$

$$q(x) = -\frac{1}{4\mu}\left(\frac{\pi a^3b^3}{a^2+b^2}\right)\frac{dp}{dx}. \tag{18}$$

The inner endothelium surface of the elliptical segment in Schlemm's canal is porous and aqueous humor percolates in it, and outer surface is non-porous. Thus, for elliptical boundary, from equation (9)

$$\frac{dq}{dx} = \frac{\pi}{2}(a+b)w(x). \tag{19}$$

From equations (11) and (18), the differential equation for evaluating the pressure is obtained by eliminating $q(x)$ and $w(x)$, which is given below:

$$\frac{d^2p}{dx^2} - m^2p(x) = -m^2P_I, \tag{20}$$

where

$$m=\left\{\frac{2\mu(a+b)\left(a^2+b^2\right)}{a^3b^3}G\right\}^{1/2}.$$

Solving equation (20) subject to the boundary conditions 13 (i)-13 (ii), we get:

$$p(x)=P_I-\frac{\cosh(mx)}{\cosh(mL)}(P_I-P_0), \tag{21}$$

$$q(x)=\frac{mL}{4\mu}\left(\frac{\pi a^3b^3}{a^2+b^2}\right)\frac{\sinh(mx)}{\cosh(mL)}(P_I-P_0), \tag{22}$$

and

$$w(x)=\frac{m^2}{2\mu(a+b)}\frac{a^3b^3}{a^2+b^2}\frac{\cosh(mx)}{\cosh(mL)}(P_I-P_0). \tag{23}$$

Minimum wall shear stress is given by:

$$\tau_{w,\,\mathrm{min}}=\frac{4\mu q(x)}{\pi a^2 b},$$

$$\tau_{w,\,\mathrm{min}}=mL\left(\frac{ab^2}{a^2+b^2}\right)\frac{\sinh(mx)}{\cosh(mL)}(P_I-P_0). \tag{24}$$

Maximum wall shear stress is obtained as:

$$\tau_{w,\,\mathrm{max}}=\frac{4\mu q(x)}{\pi a b^2},$$

$$\tau_{w,\,\mathrm{max}}=mL\left(\frac{a^2b}{a^2+b^2}\right)\frac{\sinh(mx)}{\cosh(mL)}(P_I-P_0). \tag{25}$$

Solution to the Unsteady-State Problem

The solution to the transient state problem is obtained subject to the following boundary and initial conditions,

$$\begin{gathered}u_t(a,z,t)=0,\quad u_t(y,b,t)=0,\quad u_t(y,z,0)=u_s(y,z),\\ \frac{\partial u_t}{\partial y}(0,z,t)=0,\quad \frac{\partial u_t}{\partial z}(y,0,t)=0.\end{gathered} \tag{26}$$

The first two conditions are the no-slip flow conditions and the Dirichlet boundary conditions. They mean that the flow velocity components vanish at the wall of the elliptic canal tube. The last two conditions are symmetry conditions and are of the Neumann type. These conditions express that the velocity gradients vanish at the center of the tube. The remaining one is the initial condition for the transient problem. Equation (7) together with conditions in equation (26) constitutes a linear parabolic boundary value problem.

The partial differential equation (7) subject to the conditions (26) is solved by separation of variables method,

$$u_t\left(y,z,t\right)=Y(y)Z(z)T(t). \tag{27}$$

The partial differential equation (7) with conditions (26) reduces to the following homogenous Sturm-Liouville eigenvalue problems:

$$Y''+J^2Y=0 \qquad Y'\left(0\right)=Y(a)=0, \tag{28i}$$

$$Z''+L^2Z=0 \qquad Z'\left(0\right)=Z(b)=0, \tag{28ii}$$

and

$$T'+k^2T=0 \qquad T(0)=u_s(y,z). \tag{28iii}$$

The solutions to the above eigenvalue problems are obtained in the forms:

$$Y_p=B_p\cos\frac{\left(2p+1\right)\pi y}{2a}\ ,\ \ p=0,1,2,\cdots, \tag{29i}$$

$$Z_q=D_q\cos\frac{\left(2q+1\right)\pi z}{2b}\ ,\ \ q=0,1,2,\cdots, \tag{29ii}$$

$$T_{pq}=\exp\left[-\left\{\left(\frac{(2p+1)\pi}{2a}\right)^2+\left(\frac{(2q+1)\pi}{2b}\right)^2\right\}t\right]. \tag{29iii}$$

Using the principle of superposition, the solution of the transient problem is obtained as,

$$u_t=\sum_{p=0}^{\infty}\sum_{q=0}^{\infty}D_{pq}\,cos\,\frac{(2p+1)\pi y}{2a}\,cos\,\frac{(2q+1)\pi z}{2b}\cdot\exp\left[-\left\{\left(\frac{(2p+1)\pi}{2a}\right)^2+\left(\frac{(2q+1)\pi}{2b}\right)^2\right\}t\right], \tag{30}$$

where

$$D_{p\,q} = \frac{4}{ab}\int_0^a\int_0^b u_s\,(y,z)\cos\,\frac{(2p+1)\pi y}{2a}\,\cos\,\frac{(2q+1)\pi z}{2b}\,dydz,$$

$$D_{p\,q} = \frac{8m}{\mu}\,(P_I - P_0)\,\frac{a^2b^2}{a^2+b^2}\,\frac{\sinh(mx)}{\cosh(mL)} \cdot \frac{(-1)^{p+q}}{(2p+1)(2q+1)\pi^2}\left(-1+\frac{8}{(2p+1)^2\pi^2}+\frac{8}{(2q+1)^2\pi^2}\right). \tag{31}$$

Now, the complete velocity distribution is given by:

$$u = \frac{m}{2\mu}\left(\frac{y^2}{a^2}+\frac{z^2}{b^2}-1\right)\frac{a^2b^2}{a^2+b^2}\,(P_0-P_I)\,\frac{\sinh(mx)}{\cosh(mL)}+\sum_{p=0}^{\infty}\sum_{q=0}^{\infty}D_{pq}\cos\frac{(2p+1)\pi y}{2a} \cdot\cos\frac{(2q+1)\pi z}{2b}\,\exp\left[-\left\{\left(\frac{(2p+1)\pi}{2a}\right)^2+\left(\frac{(2q+1)\pi}{2b}\right)^2\right\}t\right]. \tag{32}$$

The aqueous outflow is calculated as follows:

$$\text{q} = \iint u\,dydz,$$

$$= \iint\left[\frac{m}{2\mu}\left(\frac{y^2}{a^2}+\frac{z^2}{b^2}-1\right)\frac{a^2b^2}{a^2+b^2}(P_0-P_I)\frac{\sinh(mx)}{\cosh(mL)}+\sum_{p=0}^{\infty}\sum_{q=0}^{\infty}D_{pq}\cos\frac{(2p+1)\pi y}{2a} \cdot\cos\frac{(2q+1)\pi z}{2b}\,\exp\left[-\left\{\left(\frac{(2p+1)\pi}{2a}\right)^2+\left(\frac{(2q+1)\pi}{2b}\right)^2\right\}t\right]\right]dydz. \tag{33}$$

3. Results and Discussion

It is observed from the expression for the transient velocity, that the velocity exponentially decays with an increase of the time and tends to zero as time $t \to \infty$. Thus, after a sufficiently large time, the transient effects on the aqueous humor flow in the canal of Schlemm die out. It is evident from the expression (32) for the complete velocity that after sufficiently long time, the complete velocity resumes the steady-state velocity.

The computational results of the proposed model for the flow of aqueous humor in the canal of Schlemm have been obtained and presented through the graphs using some typical values of various model parameters listed in Table 1.

Table 1. Parameters appearing in the model and their approximate corresponding values in the human aqueous outflow network

Parameter	Description	Typical physiological value
a	Semi major axis of the elliptical channel	132 μm *
b	Semi minor axis of the elliptical channel	15 μm *
G	Filtration Constant	8.28182e-007 $mm^2 s / g$ **
2L	Length of canal between two collector channels	1.2 mm*
P_0	Pressure at the mouth of the collector channel	12 mmHg**
μ	Viscosity of aqueous humor	0.75 cp*

* Estimated and used by Ethier et al. (2004).
** Estimated and used by Tandon and Avtar (1989).

The computational results of the transient fluid velocity given by equation (32) and volume flux expressed by equation (33) were obtained at different points in the canal segment. It was observed from the computational results that variations in the velocity and volume flux due to time-variations are insignificant. This occurs due to very small values of the canal's geometric configurations i.e. semi major-axis and semi minor-axis of the elliptic canal. From these analytical observations, it may be concluded that sudden elevation in IOP does not cause significant acceleration effects on the fluid dynamics of the aqueous humor in the Schlemm's canal. Thus, no transient effects on aqueous humor flow behavior are significantly observed due to sudden elevation in IOP.

In view of the above observation and the conclusion of a study by Ethier et al. (2004) that SCE cells experience physiologically significant levels of shear stress promoting cell alignment, the computational results of the minimum wall shear stress and maximum wall shear stress have been obtained using the steady-state model solution and presented through the graphs. Also, the effects of some important model parameters on both the stresses have been displayed.

The effect of IOP on the minimum wall shear stress and maximum wall shear stress profiles is portrayed by the graphs in Figures 3(a) and 3(b), respectively. It is observed that a rise in IOP increases the minimum wall shear stress as well as maximum wall shear stress applied by flowing aqueous humor on the SCE wall. An elevation in IOP compresses the trabecular meshwork towards Schlemm's canal narrowing the canal. This causes an increase in minimum wall shear stress and maximum wall shear stress exerted by flowing aqueous humor on the SCE wall.

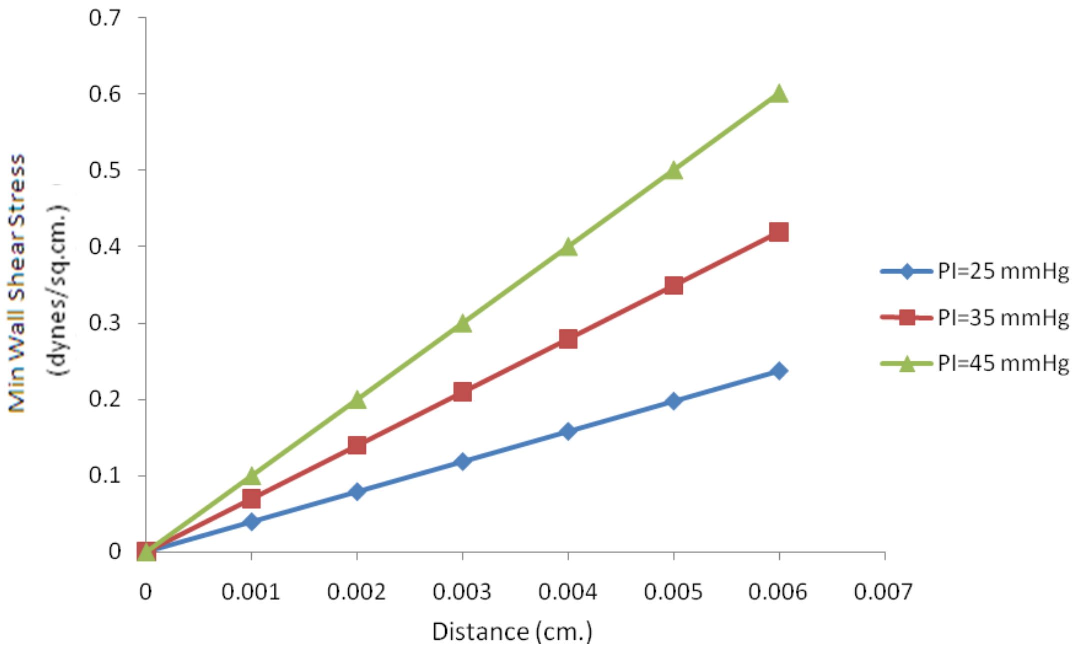

Figure 3(a). Effect of IOP on the minimum wall shear stress in the elliptic canal

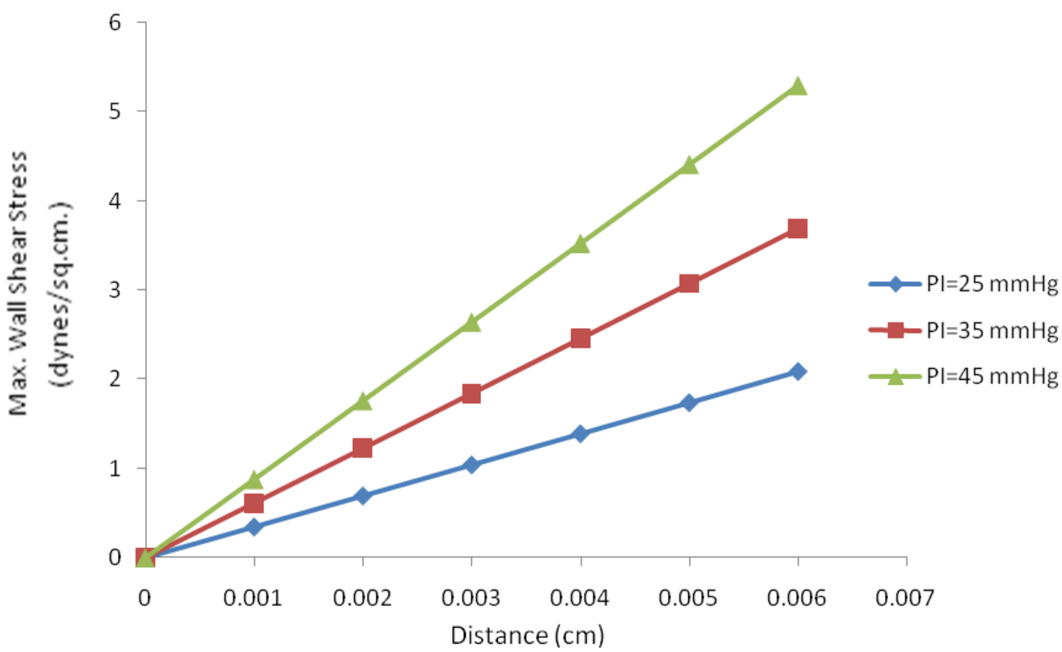

Figure 3(b). Effect of IOP on the maximum wall shear stress in the elliptic canal

The distributions of minimum wall shear stress and maximum wall shear stress in the elliptic canal segment are displayed in Figures 4(a) and 4(b), respectively. Both the stresses progress along the canal and are maximum at the collector channel ostium. As is evident from the graphs, a decrease in the filtration constant of the porous wall decreases the minimum wall shear stress and maximum wall shear stress. A decrease in the filtration constant reduces the percolation of aqueous humor in the canal of Schlemm and amount of aqueous humor reaching into the canal of

Schlemm is less and the reduced amount of flowing aqueous humor exerts less wall shear stress on the wall.

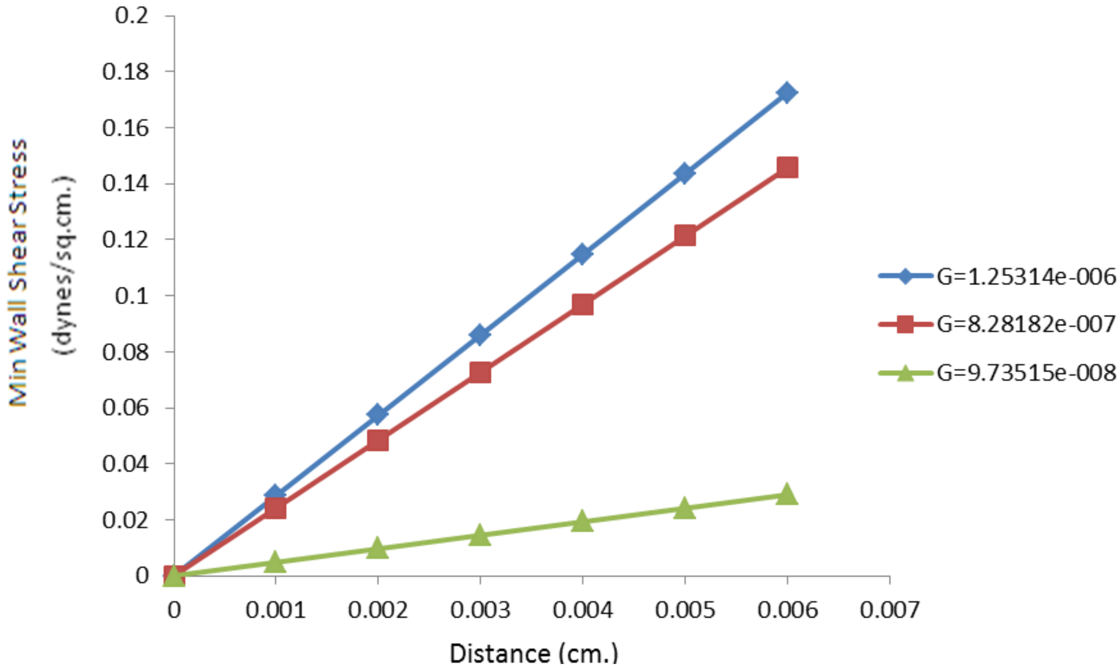

Figure 4(a). Effect of filtration constant on the minimum wall shear stress in the elliptic canal

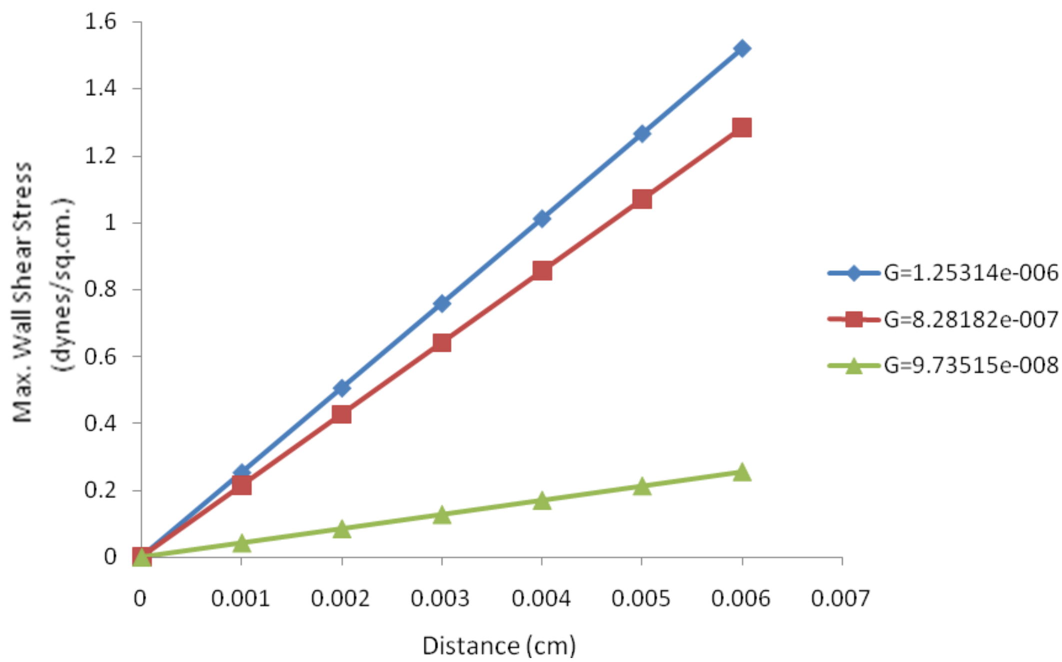

Figure 4(b). Effect of filtration constant on the maximum wall shear stress in the elliptic canal

The effect of semi-minor axis (i.e., height) of elliptic canal on the minimum wall shear stress and maximum wall shear stress profiles is shown in Figures 5(a) and 5(b), respectively. As is observed from the graphs, an increase in the semi-minor axis decreases both the minimum wall shear stress and maximum wall shear stress.

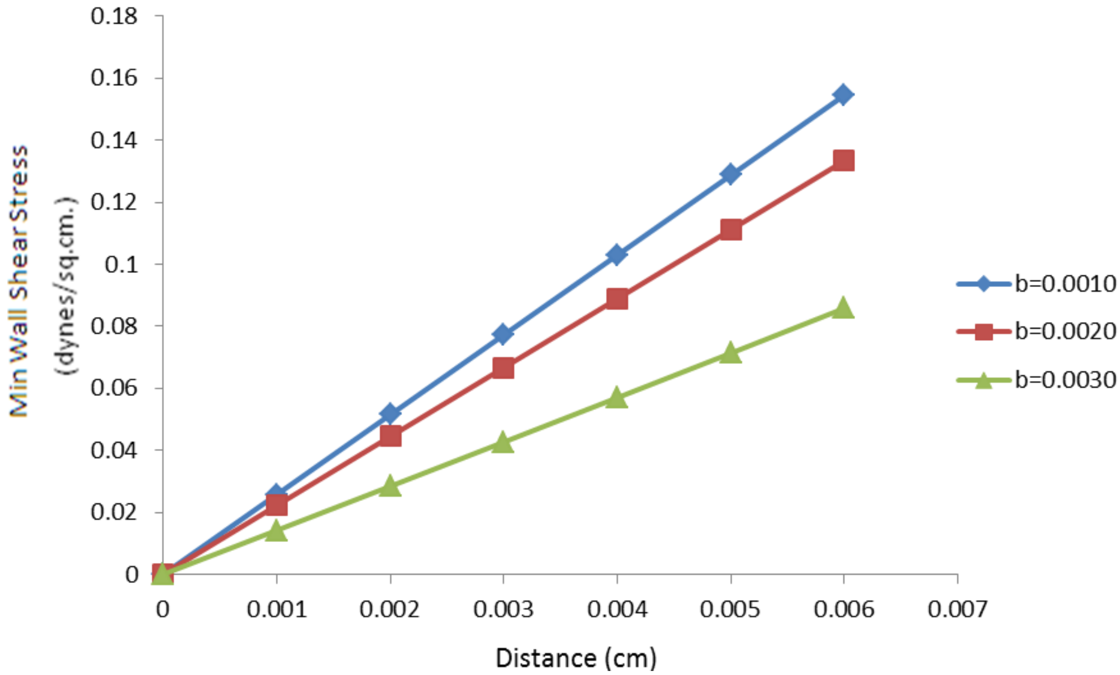

Figure 5(a). Effect of semi-minor axis on the minimum wall shear stress in the elliptic canal

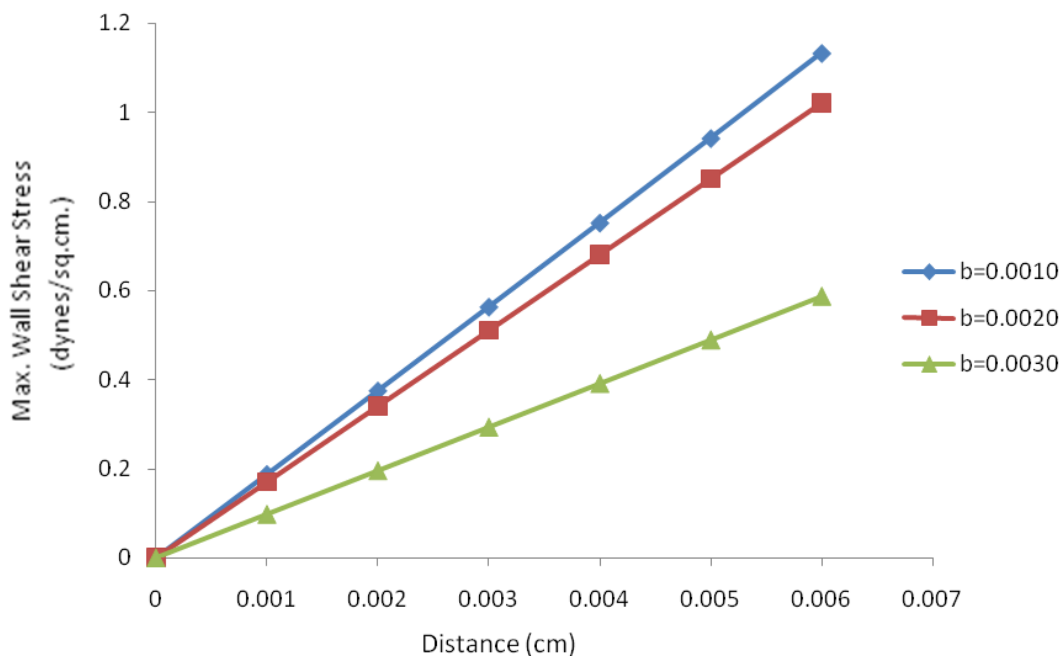

Figure 5(b). Effect of semi-minor axis on the maximum wall shear stress in the elliptic canal

The graphs in Figure 6 depict the variation in the average shear stress exerted by flowing aqueous humor on SCE wall in response to the changes in the semi-minor axis of the elliptic canal (i.e., height of Schlemm's canal). It is observed from the graphs that the average shear stress decreases with increasing the semi-minor axis (i.e., height of Schlemm's canal). It seems that increased space in the canal segment caused by an increase in the semi-minor axis reduces the average shear stress exerted by aqueous humor. Besides, the average shear stress increases along the elliptic canal segment. The average shear stress is a maximum at the collector channel ostium.

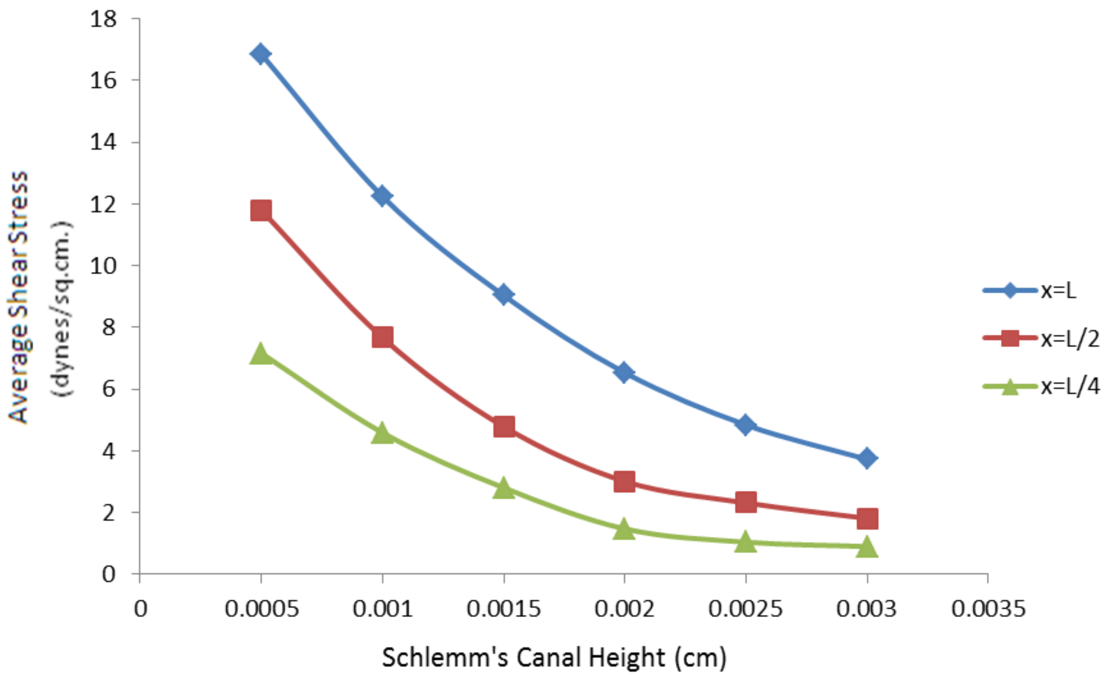

Figure 6. Variation in Average Shear Stress with change in semi-minor axis

4. Conclusion

It is concluded from the computational results obtained from the analytic expressions of the unsteady fluid velocity and aqueous volume flux that a sudden elevation in the IOP causes insignificant effects on the fluid dynamics of the aqueous humor in Schlemm's canal due to very small values of the canal's geometric configurations. In the steady-state, a rise in the IOP and an increase in the filtration constant increase the both the shear stresses exerted by flowing aqueous humor on the SCE wall. An increase in the height of Schlemm's canal decreases the minimum wall shear stress and maximum wall shear stress. The sensitivity analysis of average shear stress at the height of the elliptic Schlemm's canal leads to the conclusion that the average shear stress is a maximum at the collector channel ostium and decreases away.

The present study may be useful in the elucidation of the mechanism of cell alignment and in the determination of optimal range of values of the sufficient shear stresses which will ensure physiologically important degree of alignment of SCE cells required for normal drainage of aqueous humor through Schlemm's canal. The model results may contribute to the understanding of how SCE cells influence IOP.

Acknowledgement

The authors gratefully acknowledge the constructive comments and suggestions of Reviewers in view of which the work has been improved.

REFERENCES

Avtar, R. and Srivastava, R. (2006). Aqueous outflow in Schlemm's canal, *Applied Mathematics and Computation* 174, 316-328.

Ethier, C.R. (2002). The inner wall of Schlemm's Canal, Exp. Eye Res. Rev. 74(2), 161-172.

Ethier, C.R., Read, A.T. and Chan, D. (2004). Biomechanics of Schlemm's Canal Endothelial Cells: Influence on F-Actin Architecture, *Biophysical Journal*, 2828-2837.

Hamanaka, T., Bill, A., Ichinohasama, R. and Ishida, T. (1992). Aspects of the development of Schlemm's canal, *Exp. Eye Res*. 55, 479-488.

Ismail, Z. and Fitt, A.D. (2008).Mathematical Modelling of flow in Schlemm's Canal and its influence on Primary open angle glaucoma, International Conference on Science & Technology: *Applications in Industry & Education*.

Johnson, M.A. and Grant, W.M. (1973). Pressure dependent changes in structures of the aqueous outflow system of human and monkey eyes, *Am. J. Ophthalmol.* 75, 365-383.

Johnson, M. and Kamm, R.D. (1983). The role of Schlemm's Canal in aqueous outflow from the human eye, *Invest. Ophthalmol. Vis. Sci.* 24, 320.

Krohn, J. (1999). Expression of factor VIII-related antigen in human aqueous drainage channel, *Acta Ophthalmol. Scand.*77, 9-12.

Nesterov, A.P. (1970). Role of blockage of Schlemm's canal in pathogenesis of primary open angle glaucoma, **Am. J. Ophthalmol**. 70, 691-696.

Nesterov, A.P. and Batmanov, Y.E. (1970). Study on morphology and function of the drainage area of the eye of man, *Acta Ophthalmol*. 50, 337-350.

Tandon, P.N. and Autar, R. (1989). Flow of aqueous humor in the canal of Schlemm's, *Math. Biol. Sci.* 93, 53-78.

Van Buskirk, E.M. (1982). An atomic correlation of changing aqueous outflow of facility in excised human eyes, *Invest. Ophthalmol. Visual Sci*. 225, 625-632.